

## Supplementary Information for

### Switchable assembly and function of antibody complexes in vivo using a small molecule

Alexander J. Martinko<sup>1</sup>, Erin F. Simonds<sup>1</sup>, Suchitra Prasad, Alberto Ponce, Colton J.

Bracken, Junnian Wei, Yung-Hua Wang, Tiffany-Lynn Chow, Zhong Huang, Michael J.

Evans, James A. Wells, Zachary B. Hill\*

#### **Author Information:**

##### **Affiliations:**

Soteria Biotherapeutics, Inc., San Francisco, California, USA

Alexander J. Martinko

Erin F. Simonds

Alberto Ponce

Suchitra Prasad

Zhong Huang

Zachary B. Hill

Department of Pharmaceutical Chemistry and Department of Cellular and  
Molecular Pharmacology, University of California, San Francisco, San Francisco,  
California, USA.

James A. Wells

Department of Pharmaceutical Chemistry and Chemistry and Chemical Biology  
Graduate Program, University of California, San Francisco, San Francisco,  
California, USA.

Cole Bracken

Department of Radiology & Biomedical Imaging, University of California, San Francisco, San Francisco, California, USA.

Michael J. Evans  
Yung-Hua Wang  
Junnian Wei

---

**Present addresses:**

Present address: ArsenalBio, South San Francisco, California, USA

Alberto Ponce

Present address: Scorpion Therapeutics, South San Francisco, California, USA

Tiffany-Lynn Chow

**Corresponding author:**

Correspondence to Zachary B. Hill (zach@soteriabiotx.com)

**This PDF file includes:**

Figures S1 to S14  
Tables S1 to S2  
Extended Methods

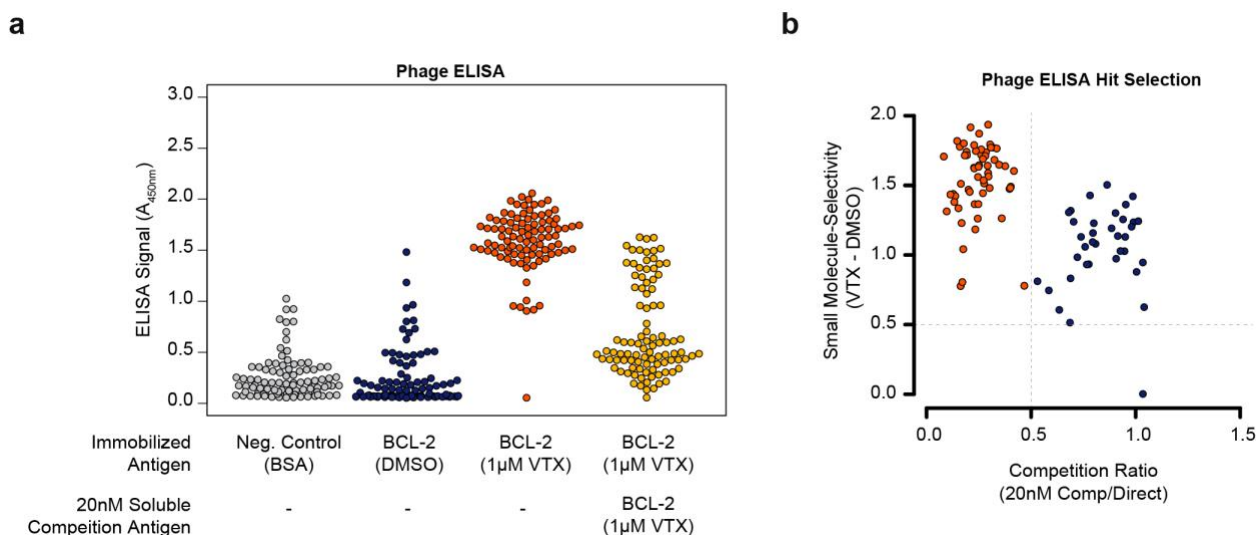


**Fig. S1. ELISA characterization of Fab-phage clones selected against the BCL-2/Venetoclax complex** (a) Fab-phage clones showed robust binding to BCL-2 in the presence of venetoclax (orange), and weak or negligible binding to BCL-2 with DMSO (blue) and BSA (grey). Binding to BCL-2 in the presence of venetoclax was competed by 20 nM of soluble BCL-2 with saturating venetoclax. The experiment was performed once without technical replicates. (b) ELISA data was analyzed to define criteria for advancement of Fab-phage clones to characterization as recombinant Fabs. Clones that showed venetoclax-dependent binding and greater than 50% competition with 20 nM competition antigen (orange) were advanced for further characterization.

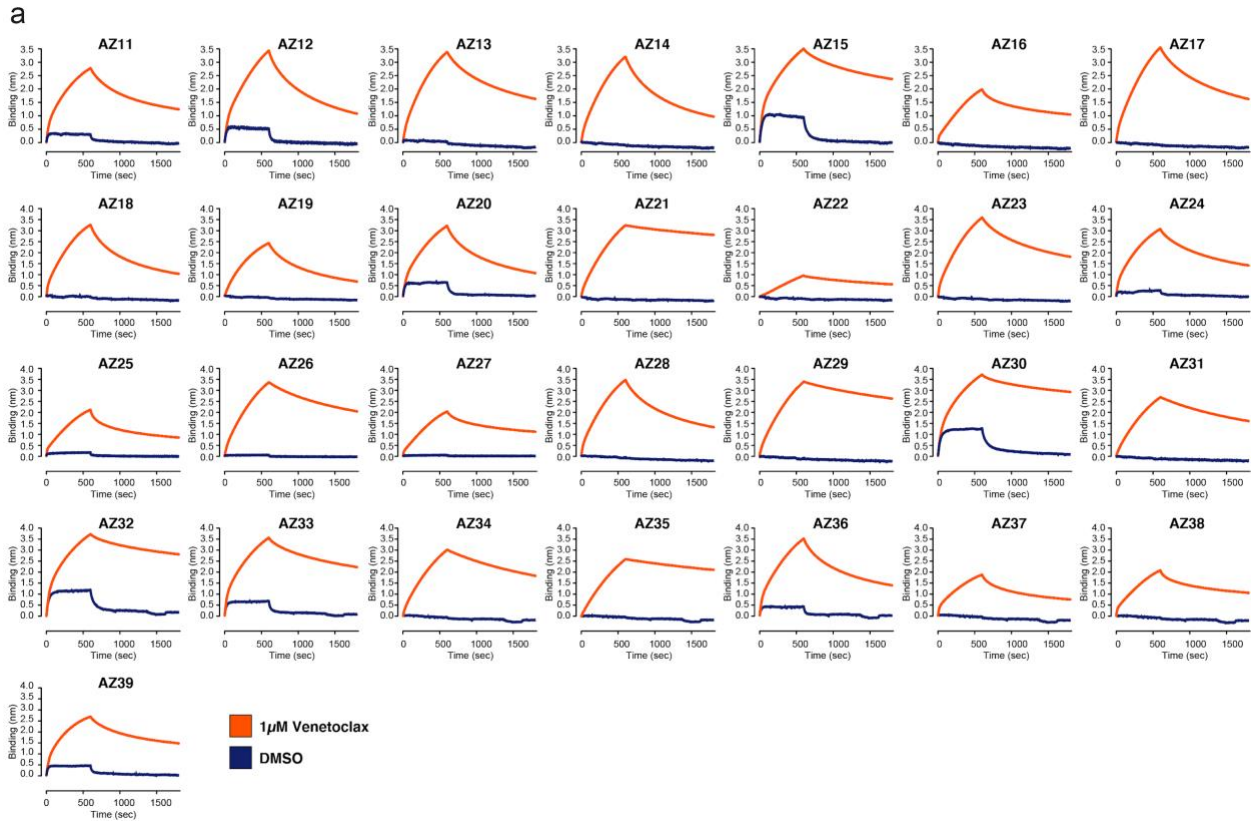


**Fig. S2. Biolayer interferometry characterization of small-molecule dependent binding of purified Fabs to BCL-2. (a)** All Fabs showed enhanced binding to BCL-2 in the presence of saturating venetoclax (orange) compared to DMSO (blue). Each curve represents a single experiment.

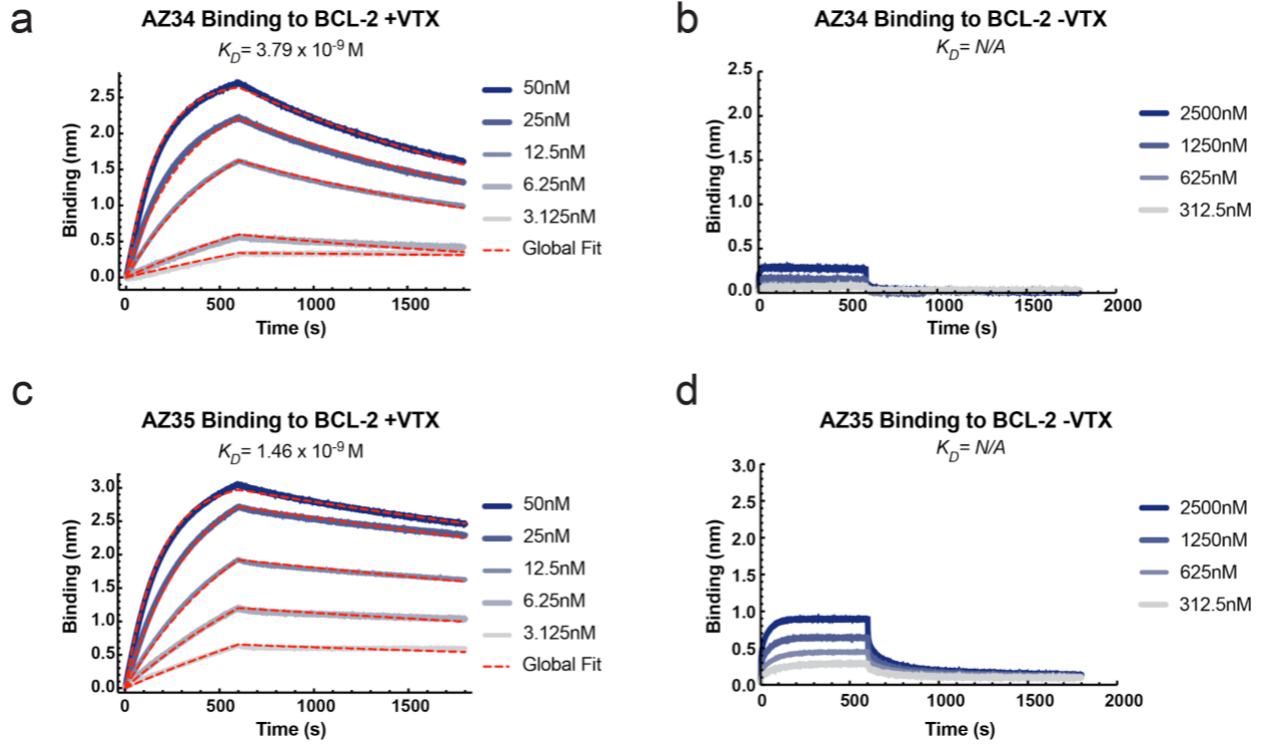


**Fig. S3. Biolayer interferometry characterization of Fab AZ34 and AZ35 binding kinetics.** (a) Fab AZ34 shows potent and reversible binding to BCL-2 in the presence of saturating venetoclax (1  $\mu\text{M}$ ) (b) and significantly weaker binding in the absence of venetoclax. (c) Fab AZ35 shows potent and reversible binding to BCL-2 in the presence of saturating (1  $\mu\text{M}$ ) venetoclax (d) and significantly weaker binding in the absence of venetoclax.

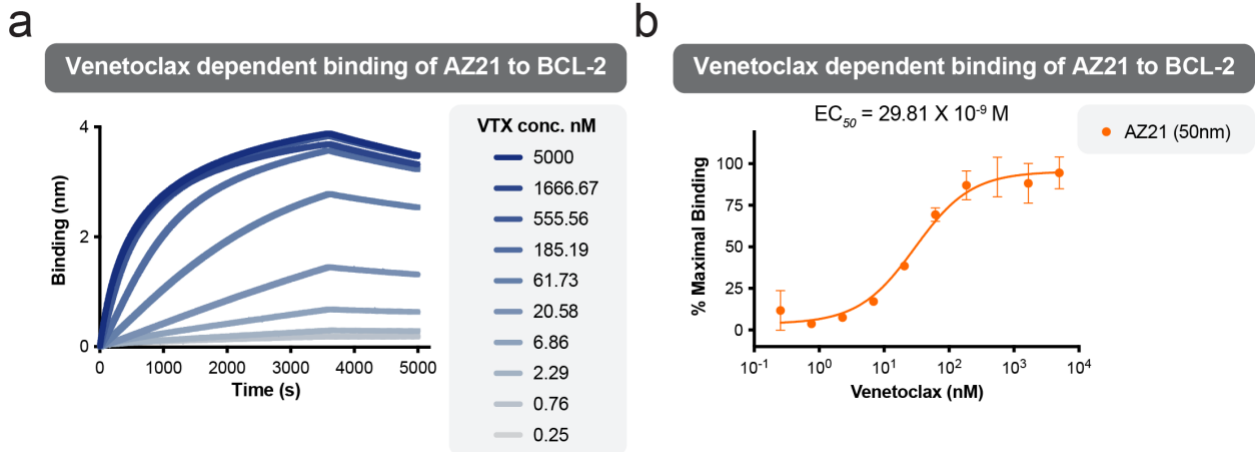


**Fig. S4. Biolayer interferometry characterization of venetoclax dependent binding kinetics of Fab AZ21.** (a) Fab AZ21 shows venetoclax dose-dependent binding to BCL-2. (b) Dose response curve for the induction of AZ21/BCL-2 dimerization by venetoclax. The binding (nm) signal for each venetoclax concentration at 3600 s was normalized as a percentage of the signal for 5000 nM venetoclax at 3600 s. As saturated binding was not achieved at the lower concentrations of ventoclax after 3600 s, the  $EC_{50}$  reported is likely higher than that which would be observed if the system were at equilibrium. Each data point represents the mean of 3 independent experiments  $\pm$  s.d. The  $EC_{50}$  was using 3-parameter nonlinear regression (error bars SEM; n = 3 per group).

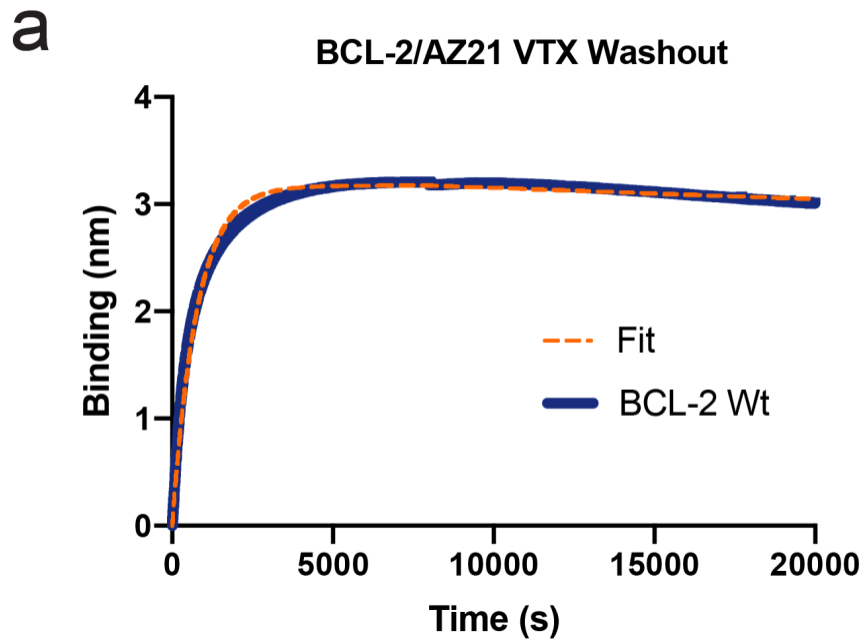


**Fig. S5. Biolayer interferometry characterization of Fab AZ21 reversibility upon infinite dilution of venetoclax. (a) Raw reversibility data corresponding to the normalized WT plot in Figure 2f.**



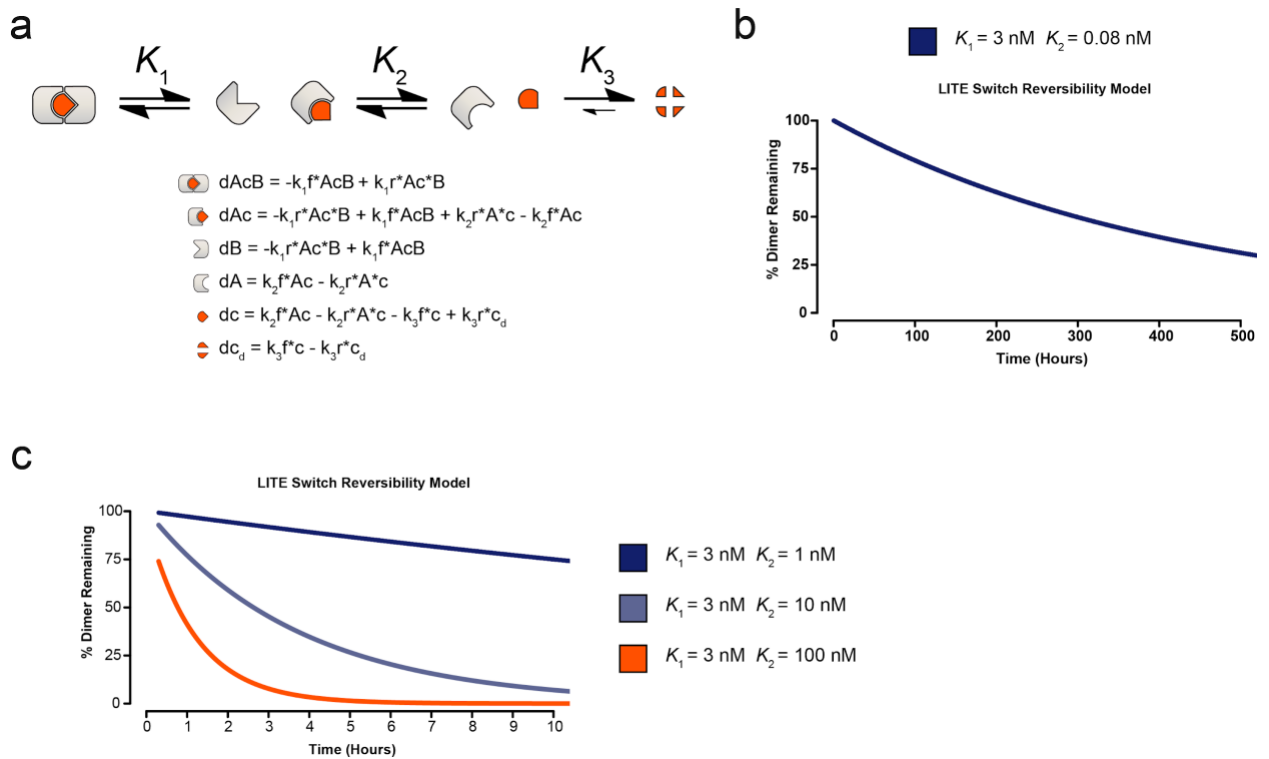


**Fig. S6. Kinetic modeling of LITE switch reversibility kinetics** (a) An ordinary differential equation model to describe the assembly and disassembly of the LITE Switch. (b) Modeling of the AZ21 dissociation from WT BCL-2 when venetoclax is removed from the system suggests reversibility kinetics on the order of several days (c) Kinetic modeling suggests that weakening the affinity of BCL-2 for venetoclax should significantly reduce the half-life of the LITE Switch when venetoclax is removed.

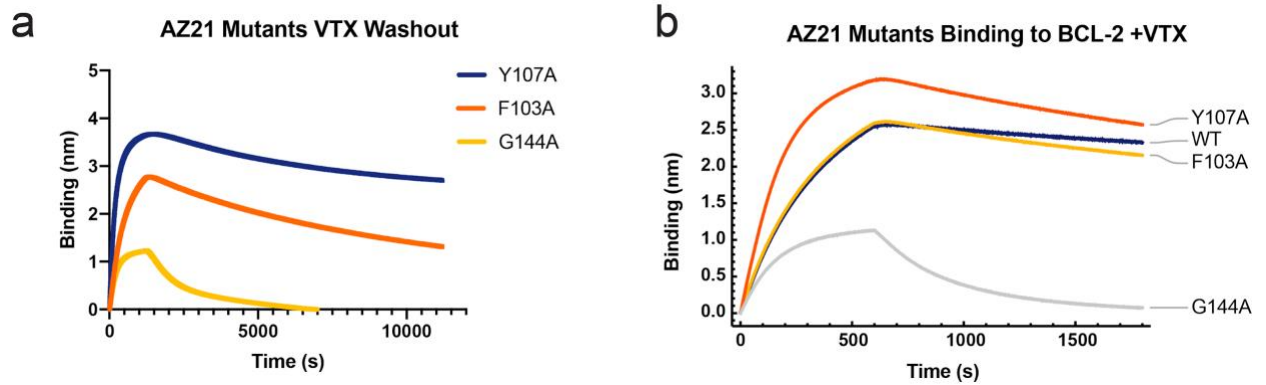


**Fig. S7. Biolayer interferometry characterization of Fab AZ21 binding to reversible mutants. (a)** Raw reversibility data corresponding to the normalized plots in Figure 1f. **(b)** AZ21 showed comparable (Y107A, F103A) or slightly reduced (G144A) binding to BCL-2 reversible mutants in the presence of saturating venetoclax (1  $\mu$ M).

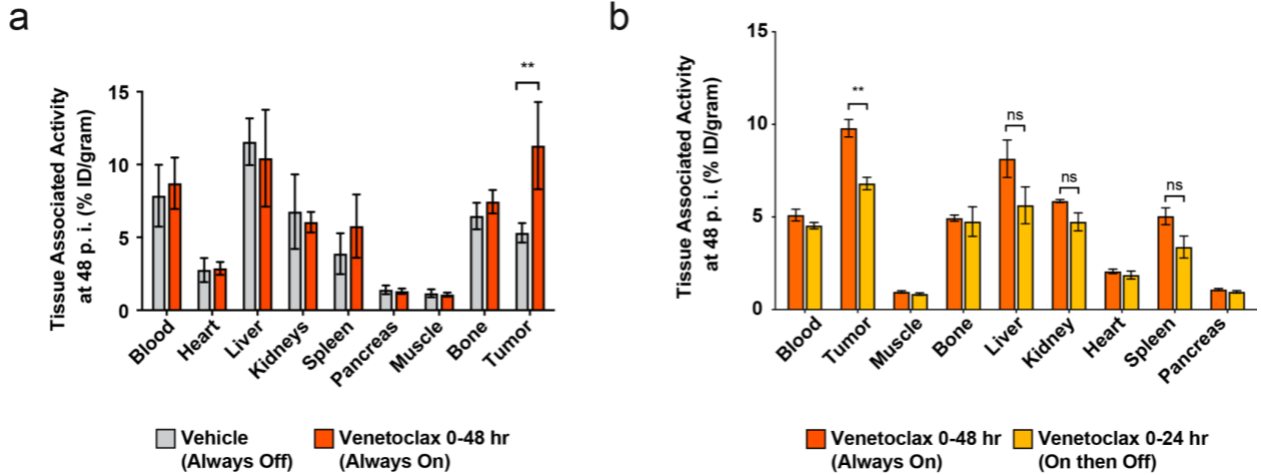


**Fig. S8. Quantified PET biodistribution data** (a) Venetoclax treatment resulted in a significant increase in tumor localized PET signal determined by *ex vivo* quantification of the biodistribution of the  $^{89}\text{Zr}$ -conjugated antibody (Ab02) in isolated tissues (error bars SEM;  $n = 4$  per group). Data corresponds to Figure 3d. (b) Tumor localization of Ab02 was significantly reversed when dosing of venetoclax was halted at 24 hours after infusion of the antibodies (error bars SEM;  $n = 4$  per group (Always On) or 3 per group (On then Off)). Data corresponds to Figure 3f.

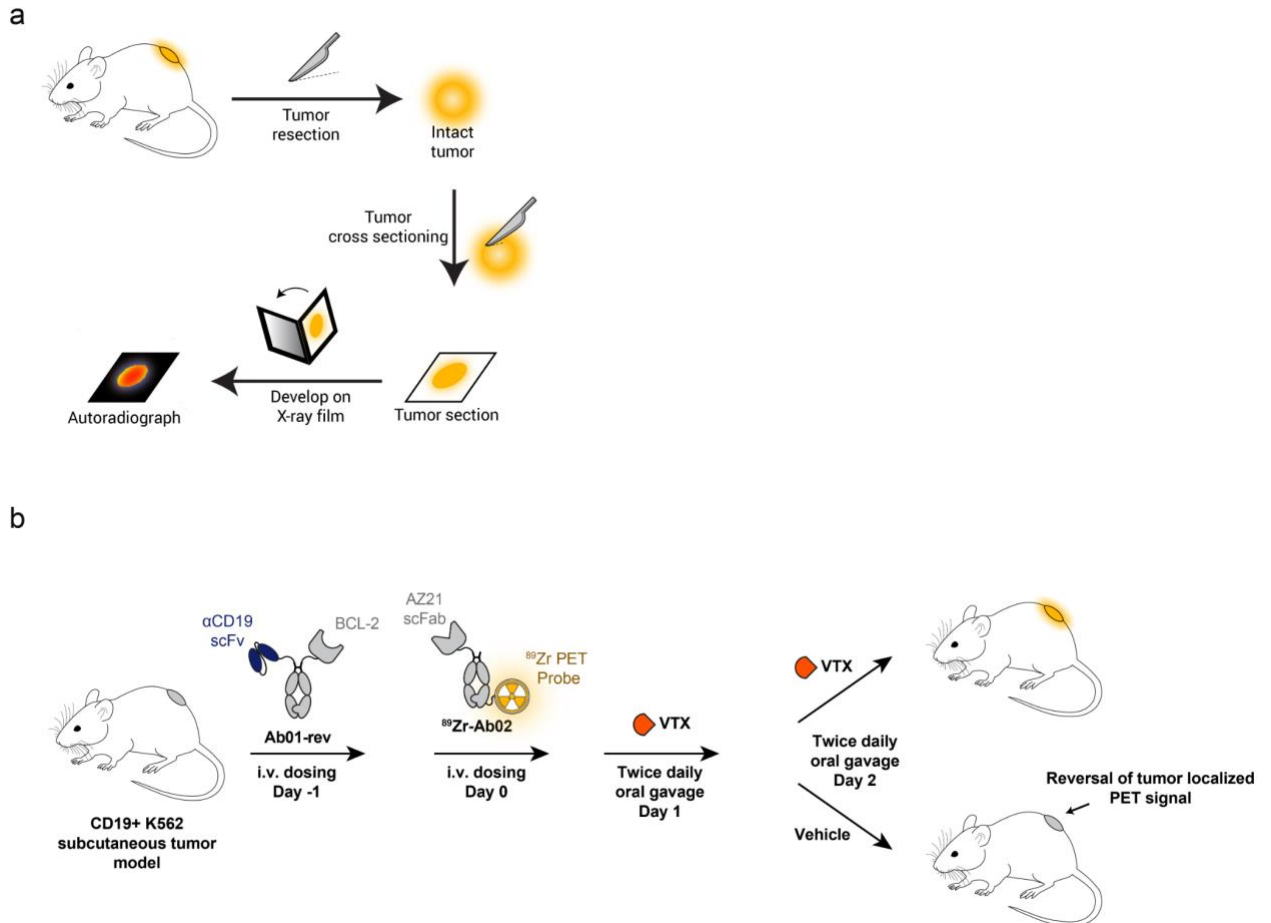


**Fig. S9. Schematic of PET autoradiography and reversibility studies (a)** Schematics of the autoradiography study experiment in Fig. 3e. **(b)** Schematic of the PET reversibility experiment described in Fig. 3f.

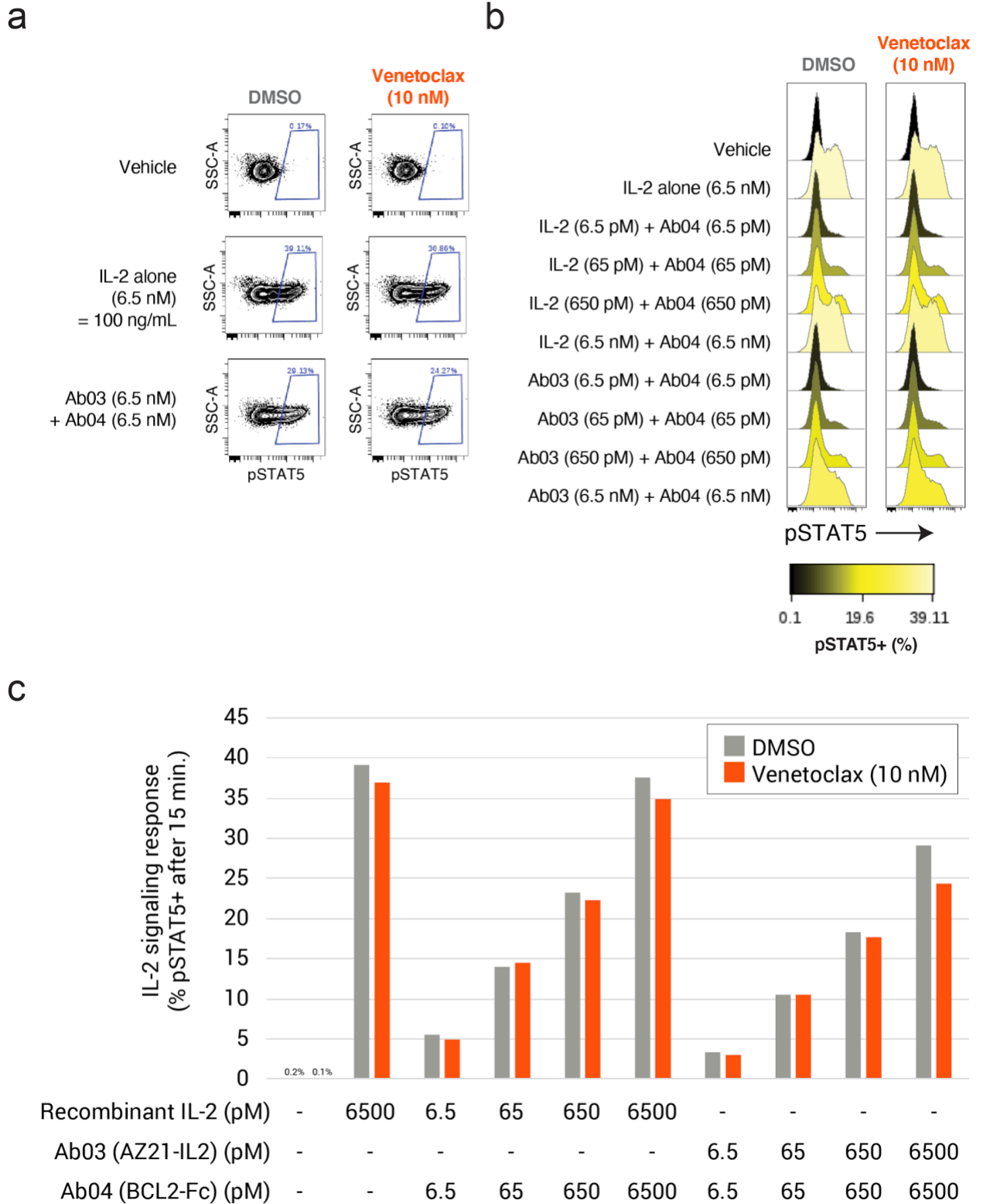
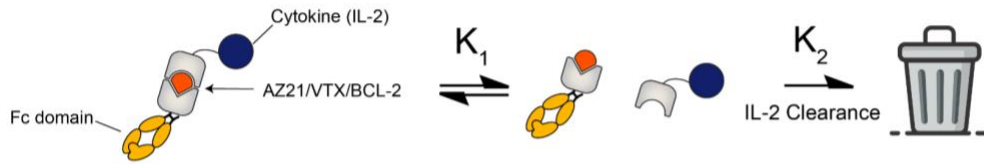


**Fig. S10. Phosphorylation of STAT5 in human T-cells treated with IL-2 or Ab03 with varying concentrations of Ab04.** (a) Representative gating strategy to quantify cells with induction of phosphorylated STAT5 (pY694) (pSTAT5+). Only singlet-gated events were

included in the analysis. Non-activated, magnetically isolated human T cells were treated with recombinant IL-2, AZ21-IL-2 (Ab03), BCL2-Fc (Ab04), venetoclax, or DMSO (Vehicle) at the concentrations indicated. After 15 minutes, cells were fixed, permeabilized, and measured with an antibody specific for pSTAT5. **(b)** Histograms show pSTAT5 intensity of each sample, shaded by the frequency of pSTAT5+ cells. Gating and analysis was performed using Cytobank software (cytobank.org). Experiment was performed once. **(c)** The frequency of pSTAT5+ cells increased in a dose-dependent fashion with increasing concentrations of recombinant IL-2 or Ab03, regardless of co-administration of Ab04 or 10 nM venetoclax. Experiment was performed once.

a



$$\begin{aligned}
 dF_cC &= -k_1f^*F_cC + k_1r^*F_c^*C \\
 dF_c &= -k_1r^*F_c^*C + k_1f^*F_cC \\
 dC &= -k_1r^*F_c^*C + k_1f^*F_c/C - k_2f^*C + k_2r^*Cd \\
 dCd &= k_2f^*C - k_2r^*Cd
 \end{aligned}$$

b

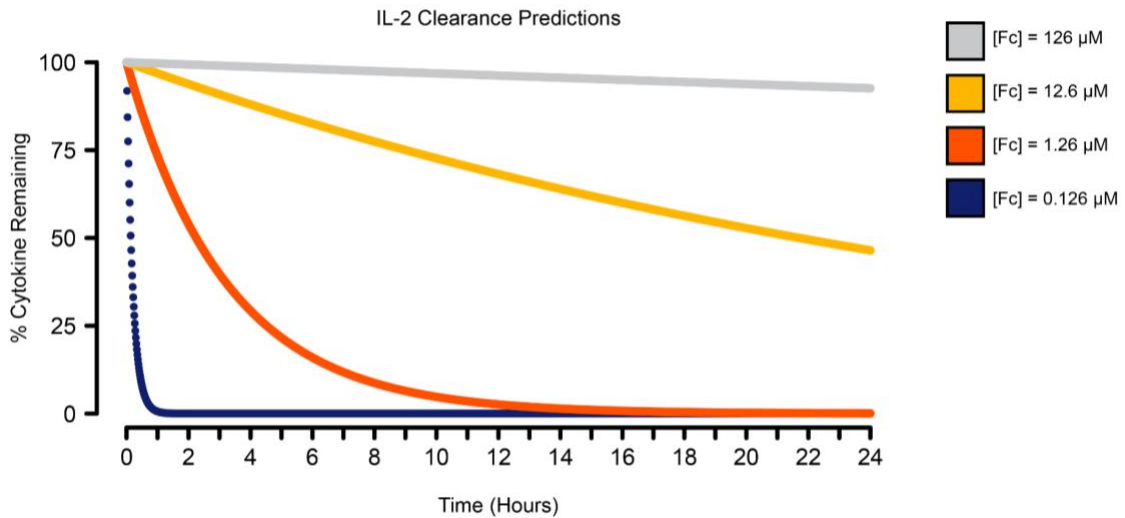


**Fig. S11. Kinetic modeling of IL-2 clearance kinetics.** (a) An ordinary differential equation model was created to describe the assembly, disassembly, and clearance of the IL-2/Fc system. (b) For therapeutic applications, we acknowledge that even more extension of half-life for IL-2 than we showed experimentally (Fig. 3d) may be necessary. Fortunately our system rapidly lends itself to this, by the ability to increase the dose of the half-life extension module (Ab04) given, relative to the therapeutic module (Ab03). Based on simple kinetic calculations, we estimate that by dosing higher with Ab04 and increasing the C<sub>max</sub> measured in our study (1.26μM) to 12.6μM, the plasma half-life of IL-2 should increase from ~144 minutes to ~ 1day through increased formation of the T-LITE complex, and therefore increased association with the Fc domain.

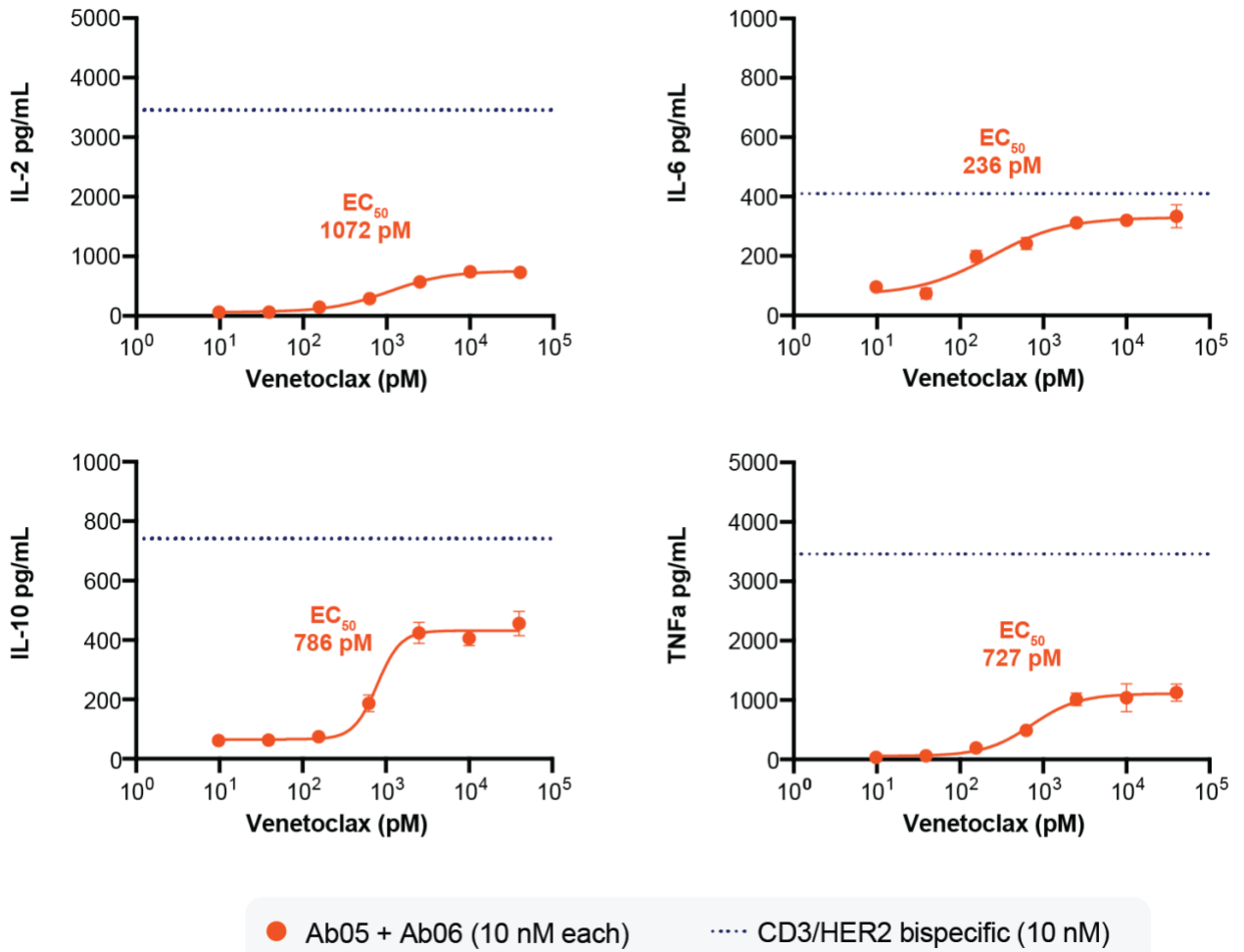


**Fig. S12. T-cell cytokine production can be regulated by venetoclax.** Secretion of IL-2, IL-6, IL-10, and TNF $\alpha$  by T-cells in a co-culture assay was chemically regulated by the concentration of venetoclax. Primary human T-cells were mixed with HER2<sup>+</sup> SKBR3 target cells at a ratio of 10:1 and treated with 10 nM of T-LITE antibodies (Ab05 and Ab06) at varying concentrations of venetoclax for 70 hours. Error bars SEM; n=3 technical replicates.



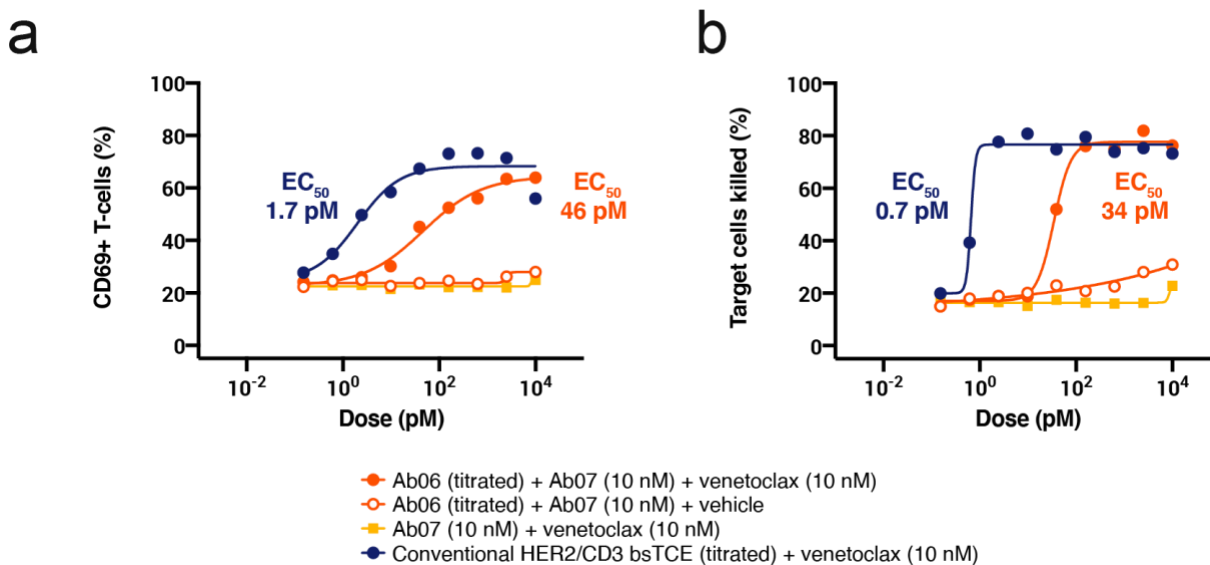
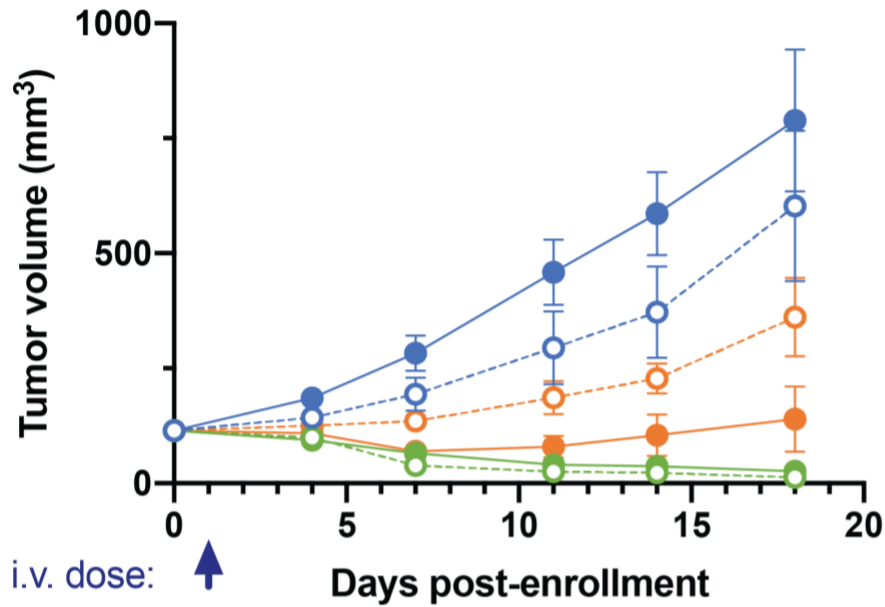


**Fig. S13. T-cell activation and redirected killing of HER2+ tumor cells can be potently induced by a chemically regulated bispecific T-cell engager *in vitro*.** (a) The HER2/CD3 T-LITE potently activated T-cells in a co-culture assay as measured by flow cytometry quantification of CD69 cell-surface staining. Non-activated primary human T-cells were mixed with SKBR3 target cells at a ratio of 10:1 and treated with T-LITE antibodies with and without venetoclax at the indicated concentrations for 69 hours. No activation was observed in the absence of venetoclax (*open orange circles*) or when only the anti-CD3 T-LITE Ab was added (*yellow squares*). A conventional HER2/CD3 bispecific T-cell engager (bsTCE; *blue circles*) was included as a positive control. Data represents the mean of n=3 technical replicates. (b) The HER2/CD3 T-LITE potently induced T-cell-dependent cellular cytotoxicity (TDCC) of HER2+ SKBR3 tumor cells in a dose-dependent fashion, and only in the presence of venetoclax. Data represents the mean of n=3 technical replicates.



- Gr. 01: Vehicle (-VTX)
- Gr. 02: Vehicle (+VTX)
- Gr. 03: T-LITE (1 mg/kg M.E.) (-VTX)
- Gr. 04: T-LITE (1 mg/kg M.E.) (+VTX)
- Gr. 05: Conventional bispecific (1 mg/kg M.E.) (-VTX)
- Gr. 06: Conventional bispecific (1 mg/kg M.E.) (+VTX)

**Fig. S14. Response to treatment in smaller tumors in the HER2 T-LITE efficacy study.** In the same BT-474 + PBMC admixed xenograft experiment shown in Figure 5, six additional groups of mice were enrolled with smaller tumors (100 mm<sup>3</sup> instead of 150 mm<sup>3</sup>). In these smaller tumors, venetoclax (VTX) treatment on its own trended toward increasing tumor growth, presumably by suppressing T-cell activation (compare Gr. 01 and Gr. 02). However, when T-LITE antibodies were co-administered, this immunosuppressive effect of venetoclax was overcome by the anti-tumor effect of the T-LITE (compare Gr. 03 and Gr. 04). The conventional bispecific caused potent tumor regression regardless of venetoclax treatment. Doses were scaled to molar equivalents (M.E.) of a standard IgG antibody. The 1 mg/kg M.E. T-LITE dose corresponds to the 0.8 mg/kg dose shown in Figure 5. Error bars SEM; n=5 per group.

**Table S1** Differential Scanning Fluorimetry of Fab fragments and BCL-2 in the presence of Venetoclax. Fabs showed no T<sub>m</sub> shift greater than 1.5 °C in the presence of venetoclax, supporting that they do not bind Venetoclax in the absence of BCL-2. In contrast, BCL-2, which showed a 22.4 °C increase in T<sub>m</sub> in the presence of venetoclax. The control Fab is an isotype control selected against an unrelated target with identical framework to AZ11-39 but differing CDR sequences. Each data point represents the mean of 3 independent experiments. Instrument measurement co-variation was determined to be ± 0.29 °C.

Protein	AZ11	AZ12	AZ13	AZ14	AZ15	AZ16	AZ17	AZ18	AZ19	AZ20	AZ21	AZ22	AZ23	AZ24	AZ25	AZ26	AZ27	AZ28	AZ29	AZ30	AZ31	AZ32	AZ33	AZ34	AZ35	AZ35	AZ37	AZ38	AZ39	Ctrl Fab	BCL2
T <sub>m</sub> (°C) (0.2% DMSO)	79.0	81.1	78.8	73.1	77.7	72.2	76.2	75.4	77.4	77.1	80.3	79.5	77.9	79.1	81.6	82.1	72.3	76.8	81.9	80.4	79.7	80.1	80.0	79.9	77.4	80.2	78.7	74.5	77.8	79.9	59.1
T <sub>m</sub> (20 μM VTX)	79.8	81.9	79.6	73.4	79.1	73.2	77.6	76.3	78.1	77.6	81.7	80.0	78.6	80.1	83.1	83.3	73.3	77.5	83.1	81.5	80.9	81.2	81.3	81.0	78.7	81.3	79.9	75.6	78.5	80.9	81.4
ΔT <sub>m</sub> (°C)	0.8	0.8	0.8	0.2	1.4	1.0	1.5	0.9	0.7	0.6	1.4	0.5	0.7	1.0	1.5	1.1	1.0	0.6	1.2	1.1	1.3	1.1	1.3	1.2	1.3	1.0	1.2	1.1	0.7	0.9	22.4

**Table S2.** Binding and kinetic constants measured for binding of Fabs AZ21, AZ34, and AZ35 to BCL-2 in the presence or absence of venetoclax. N.D. indicates the values could not be determined because binding was not detected.

Fab ID	VTX 1 $\mu$ M	$K_D$ ( $10^{-9}$ M)	$k_{ON}$ ( $10^5$ M $^{-1}$ s $^{-1}$ )	$k_{OFF}$ ( $10^{-4}$ s $^{-1}$ )
AZ21	+	1.79	0.43	0.76
	-	>5000	N.D.	N.D.
AZ34	+	3.79	1.15	4.35
	-	>5000	N.D.	N.D.
AZ35	+	1.46	1.06	1.55
	-	>5000	N.D.	N.D.

## **Extended Methods:**

### **Phage ELISA**

ELISAs were performed according to standard protocols. Briefly, 384-well Maxisorp plates (Nunc) were coated with NeutrAvidin (10 µg/mL) overnight at 4 °C and subsequently blocked with BSA (2% w/v) for 1 h at 20 °C. 20 nM of biotinylated BCL-2 was captured on the NeutrAvidin-coated wells for 30 min and was followed by the addition of phage-containing bacterial supernatants diluted 1:5 in PBS + 0.05% Tween + 0.2% BSA with 1 µM venetoclax, 1 µM venetoclax + 25 nM of BCL-2, or 0.05% DMSO for 20 min. The bound Fab-phage were then detected using a horseradish peroxidase (HRP)-conjugated anti-M13 monoclonal antibody (GE Lifesciences: 27-9421-01).

**Differential Scanning Fluorimetry (DSF).** DSF was performed on a LC480 Lightcycler Instrument II (Roche). Purified recombinant protein was diluted to 5 µM in DSF buffer (PBS, pH 7.4, Sypro Orange 5×) with small molecule (10 µM VTX) or vehicle (0.05% DMSO) and then heated with a temperature gradient (0.01 °C/s) from 25 to 95 °C. Data were continuously acquired at ~465 nm (excitation) and ~580 nm (emission). Data was analyzed to generate first derivative curves in which the curve maximum was reported as the melting temperature of the protein.

### **Fab expression and purification**

Fabs were subcloned from the Fab-phagemid into an *E. coli* expression vector. All constructs were sequence-verified by Sanger sequencing. Fab constructs were then expressed in *E. coli* C43(DE3) Pro+ using optimized autoinduction medium and purified by protein A affinity chromatography as previously described.<sup>21</sup> All proteins were buffer-

exchanged into PBS by spin concentration and stored at 4°C. The purity and integrity of proteins was verified by SDS-PAGE and intact mass spectrometry (Xevo TQ-XS).

### **Antibody Expression and Purification**

All antibodies were expressed and purified from Expi293F (Thermo Fisher Scientific) or modified Expi293 BirA-KDEL<sup>22</sup> cells according to an established protocol from the manufacturer (Thermo Fisher Scientific). Culturing media for BirA cells was additionally supplemented with 100 µM of biotin prior to transfection for *in vivo* biotinylation. Fc-fusion proteins were purified by Protein A (MabSelect Prisma) affinity chromatography and His-tagged proteins were purified by Ni-NTA (Roche cOmplete™ His-Tag Resin) affinity chromatography. Eluted proteins from affinity purification were further separated by Size-exclusion chromatography with a Superdex 200 increase 10/300 GL column (Cytiva) in storage buffer (1X HBS + 5% Glycerol) as an aqueous phase. Purity and integrity were assessed by SDS-PAGE with 4-12% BIS-TRIS precast gels (Thermo Fisher Scientific).

### **Vector Generation for Antibody Expression**

Plasmids for antibody expression were constructed by standard molecular biology methods. All DNA fragments were synthesized by IDT Technologies or Twist Biosciences and subcloned into the pFUSE vector (InvivoGen) with Gibson assembly.

**Coupling of the bifunctional chelate:** In general, a solution of 1 mg of the antibody (Ab02) was diluted into 500 µL of 0.1 M sodium bicarbonate buffer (pH 9.0). *p*-Isothiocyanatobenzyl-desferrioxamine (Df-Bz-NCS) was dissolved in DMSO at a

concentration of 10 mM. 10  $\mu$ L of the solution of Df-Bz-NCS was added dropwise to the solution of the antibody. After slow addition, the reaction was incubated for 30-45 min at 37° C. The reaction mixture was purified via a G-25 column pre-equilibrated by 10 ml of 0.2 M ammonium acetate. DFO-Ab was eluted by the 0.2 M ammonium acetate solution, the 0.7-1.4 mL portion was collected and measured the concentration for the next labelling step, and the yield of DFO labelling is typically > 90%.

**Radiochemistry:** In general, a solution of  $^{89}\text{Zr}$ -oxalic acid (4mCi; 12  $\mu$ L) was first adjusted with 2 M  $\text{Na}_2\text{CO}_3$  (5.4  $\mu$ l). Then 100  $\mu$ L of 0.5 M HEPES was added into the reaction vial to adjust the pH to 7.0. A solution of DFO-Ab02 (0.8 mg) in 400  $\mu$ L of 0.2 M ammonium acetate was added. After incubation at room temperature for 1 h, reaction progress was determined with iTLC using a 20 mM citric acid mobile phase. The reaction routinely proceeded to >85% completion by iTLC within 1 h. The reaction mixture was purified via a G-25 column pre-equilibrated by 10 mL of 0.2 M ammonium acetate.  $^{89}\text{Zr}$  labelled Ab02 was eluted by the 0.2 M ammonium acetate solution, the 0.7-1.3 mL portion was collected, and this portion was purified again by a G-25 column pre-equilibrated with 10 mL of 0.5 M HEPES.  $^{89}\text{Zr}$  labelled Ab02 was eluted by the 0.5 M HEPES buffer and the 0.7-1.3 mL portion was collected for the animal study. Typically 2.8-3.2 mCi was obtained after the two purifications. And the specific activity of the  $^{89}\text{Zr}$ -Ab02 was around 4-5  $\mu$ Ci/mg.

### **Isolation of T cells for in vitro assays**

Leukapheresis packs were obtained from deidentified healthy adult donors (StemCell Technologies, Vancouver, BC). Peripheral blood mononuclear cells (PBMCs) were first isolated using the EasySep Direct Human PBMC Kit (StemCell Technologies). Human T

cells were magnetically isolated from the PBMCs using the EasySep Human T cell Isolation Kit (StemCell Technologies). T cells were cryopreserved in DMEM with 10% FBS and 10% DMSO and thawed the day of experiments.

### **Culturing of Cell Lines**

SK-BR-3 (SKBR3) human breast cancer cells were obtained from ATCC and maintained in DMEM with 10% fetal bovine serum and 1x penicillin/streptomycin. Cells were not expanded for fewer than 20 passages before use in assays. BT-474 cells were obtained and expanded by Crown Bioscience (Taicang, China).

### **Quantitation of STAT5 Phosphorylation**

Dilutions of recombinant human IL-2 (Peprotech, Rocky Hill, NJ), Ab03+Ab04, or Ab04 alone were prepared in growth media in V-bottom polystyrene 96-well assay plates. Either DMSO or venetoclax was added and assay plates were warmed to 37°C for at least 10 minutes prior to adding cells. Magnetically isolated human T cells were thawed, labeled with a fixable live/dead stain (CF405M, 1  $\mu$ M, 10 minutes at 37°C) (Biotium, Fremont, CA), then washed and resuspended in warm media prior to use. T cells were aliquoted to the drug dilution plate (100,000 cells per well) and incubated 15 min at 37°C. Methanol-free paraformaldehyde (Electron Microscopy Sciences, Hatfield, PA) was added to a final concentration of 1.5% for 10 minutes at room temperature. Cells were spun (600 rcf, 3 min) and resuspended in flow cytometry staining buffer (AutoMACS Running Buffer, Miltenyi Biotec GmbH, Germany) to wash. A second wash was performed and pellets were disrupted by vortexing. Ice-cold 100% methanol was added for 10 min at 4°C, followed by an equal volume of PBS, and then an equal volume of flow cytometry staining buffer. Two



washes were performed as above. Cells were resuspended and stained with PE-conjugated anti-STAT5 (pY694) (clone 47/Stat5) (BD Biosciences, San Jose, CA) at a 1:20 final dilution for 30 minutes at room temperature, then washed twice as above. Data was collected on a MACSQuant Analyzer 10 (Miltenyi Biotec) flow cytometer and analyzed using Cytobank software (Cytobank Inc., Mountain View, CA).